The following publication Lai, W. F., Hu, C., Deng, G., Lui, K. H., Wang, X., Tsoi, T. H., ... & Wong, W. T. (2019). A biocompatible and easy-to-make polyelectrolyte dressing with tunable drug delivery properties for wound care. International Journal of Pharmaceutics, 566, 101-110 is available at https://doi.org/10.1016/j.ijpharm.2019.05.045.

A biocompatible and easy-to-make polyelectrolyte dressing with tunable drug delivery properties for wound care

Abstract

Chitosan (CS) is a biodegradable and biocompatible polysaccharide which displays immune-stimulatory effects and anti-bacterial properties to facilitate wound closure. Over the years, different CS-based dressings have been developed; however, most of them are not fully biodegradable due to the involvement of synthetic polymers during dressing fabrication. In addition, preparation of many of these dressings is laborious, and may impose damaging effects on fragile therapeutic molecules. The objective of this study is to address these problems by developing a tunable, biocompatible, and biodegradable CS-based dressing for wound treatment. The dressing is fabricated via electrostatic interactions between CS and carmellose (CM). Its swelling properties, erosion behavior, loading efficiency and drug release sustainability can be tuned by simply changing the CS/CM mass-to-mass ratio. Upon loaded with minocycline hydrochloride, the dressing effectively protects the wound in mice from infection and enhances wound closure. Regarding its high tunability and promising *in vivo* performance, our dressing warrants further development as a user-friendly dressing for use in wound care.

1. Introduction

Chitosan (CS) displays good biocompatibility and immune-stimulatory effects (De Souza et al., 2009). It also facilitates tissue repair and wound closure (Jayakumar et al., 2011), and shows anti-microbial activity against diverse pathogens (including bacteria (Escarcega-Galaz et al., 2018), filamentous fungi (Roller & Covill, 1999), and yeasts (Pena et al., 2013)). In particular, CS effectively acts against gram-positive and gram-negative bacteria (Perinelli et al., 2018), with low toxicity shown in mammalian cells. These properties render CS favorable to be exploited as a dressing for offering a moist environment for wound healing while protecting the wound from bacterial infection. Over the years, different CS-based dressings have been developed (Augustine et al., 2019, Hashemi Doulabi et al., 2018, Li et al., 2018, Tamer et al., 2018). For instance, a hydrogel fabricated from CS and poly(vinyl alcohol) (PVA)

has previously been adopted to generate a minocycline-loaded dressing. The dressing has been found to suppress bacterial proliferation, to maintain a moist environment over the wound bed, and to enhance collagen proliferation in the wound area (Zhang et al., 2015). More recently, temperature-responsive polyelectrolyte complexes have been generated from poly(N-isopropyl acrylamide) and thiolated CS for sustained release of ciprofloxacin. These complexes have been found to suppress bacterial proliferation (Mishra et al., 2017). All these have corroborated the practical potential of CS-based dressings in wound management.

Many of the reported CS-based dressings in the literature, however, involve the use of synthetic polymers (e.g., PVA and poly(N-isopropyl acrylamide)), which are poorly biodegradable, during dressing fabrication. In addition, generation of most of those dressings relies on crosslinking induced by chemical triggering, radiation grafting, or freeze–thaw processing. Many of these processes are not only laborious and time-consuming, but may also damage fragile therapeutic molecules if drug loading is performed at the time of dressing fabrication. All these have complicated the preparation and use of these dressings in the clinical context. Development of an easy-to-make, fully biocompatible polyelectrolyte dressing, which on one hand can retain the bioactivity of the loaded drug and on the other hand can sustain drug release, is in dire need. The objective of this study is to meet this need by reporting a tunable CS/carmellose (CM) polyelectrolyte dressing as a sustained drug delivery system for wound healing applications (Fig. 1). CM is selected to complex with CS because it is widely used as a food additive. Along with the track record of biomedical use of CM in the literature (Ogushi et al., 2007, Pal et al., 2006, Spera et al., 2017, Vinklarkova et al., 2017, Wang et al., 2019), the biocompatibility and safety of CM are guaranteed. Compared with solutions of other anionic polysaccharides such as xanthan gum and alginate, the CM solution has been reported to be more effective in preventing the sedimentation of mixed agents (Molla et al., 2007). This enables the formation of a more homogenous dressing in which drug molecules are distributed more evenly. In this study, formation of the dressing is mediated simply by electrostatic interactions between amine groups of CS and carboxyl groups of CM. This allows the dressing to be made merely by having the two polymer solutions to be mixed right before application. Fabrication of the dressing, therefore, is simple and convenient. Finally, the swelling properties and erosion behavior, and hence the drug release sustainability, of the dressing can be easily tuned by moderating the CS/CM mass-to-mass ratio. This allows

the drug release profile given by the dressing to be tailored to meet the needs of different situations.

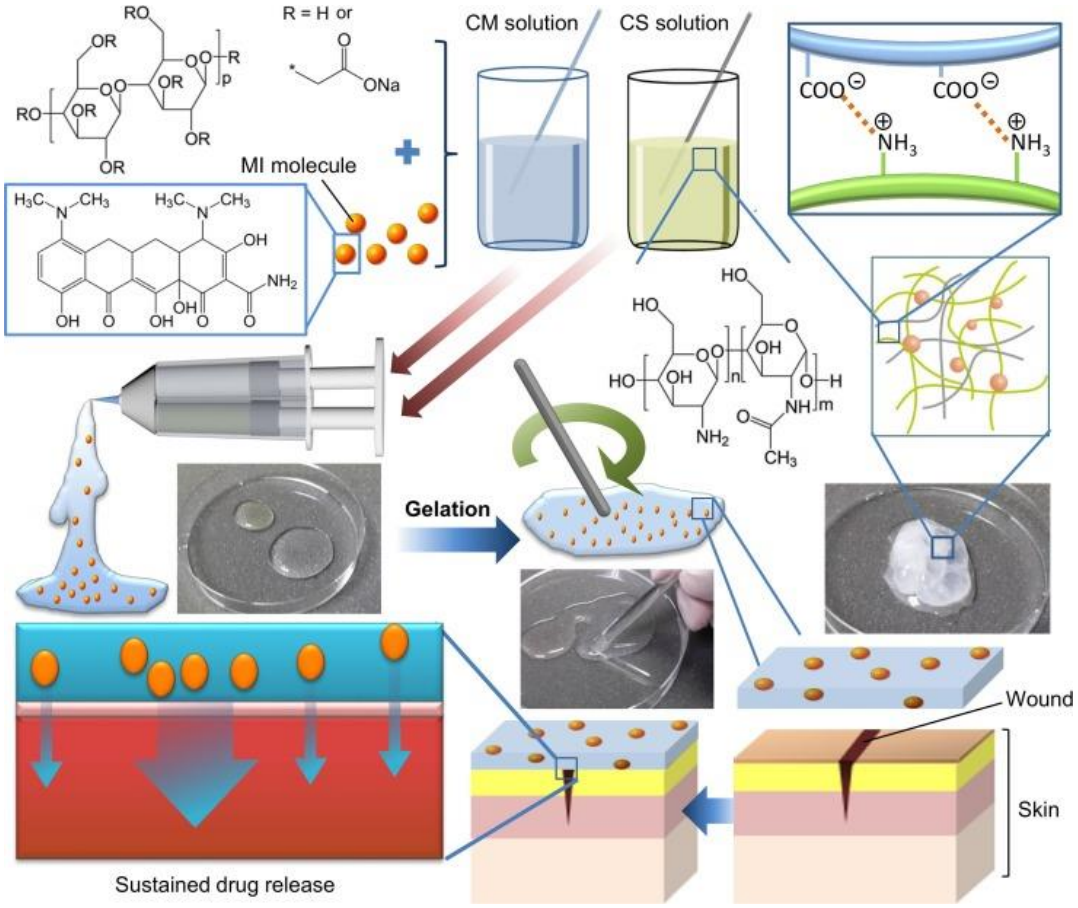

Fig. 1. A schematic diagram depicting the generation and use of the dressing in wound treatment. Abbreviation: CM carmellose; CS chitosan; MI minocycline hydrochloride.

2. Materials and methods

2.1. Materials

Methylene blue (MB), minocycline hydrochloride (MI), tetracycline hydrochloride (TH), CS (75–85% deacetylated, with the viscosity of its 1% (w/v) solution in 1% (v/v) acetic acid at 25 °C being 200–800 cP), and the sodium salt of CM (average Mw ~ 250,000, degree of substitution = 0.7) were purchased from Sigma-Aldrich (St. Louis, MO, USA). Dulbecco's Modified Eagle's Medium (DMEM; Gibco, Grand Island), penicillin G-streptomycin sulfate (Life Technologies Corporation. USA), and fetal bovine serum (FBS, Hangzhou Sijiqing Biological Engineering Materials

Co. Ltd., PR China) were used as the cell culture medium. Trypsin-EDTA (0.25% trypsin-EDTA) was obtained from Invitrogen (California, USA).

2.2. Preparation of the CS/CM (CC) dressing

CS was dissolved in 5% (v/v) acetic acid to reach a concentration of 4% (w/v). The CC dressing at the CS/CM mass-to-mass ratio of 1:8 was prepared by mixing one portion of the CS solution with 8 portions of a 4% (w/v) aqueous solution of CM. The mixture was left at ambient conditions for 5 min for gelation to occur. The dressing produced contained 11% of CS by mass, and was designated as CC_{11}. The same approach was adopted to generate CC_{03} and CC_{33}, in which the CS/CM mass-to-mass ratio adopted was 1:32 (CS mass percentage: 3.0%) and 1:2 (CS mass percentage: 33%), respectively.

2.3. Thermogravimetric analysis (TGA)

TGA of CS, CM and the lyophilized CC dressing was carried out using a Q50 TGA system (TA Instruments, New Castle, Delaware, USA) equipped with platinum pans. The measurement was performed in an inert atmosphere of nitrogen from 40 °C to 600 °C. The heating rate was uniform in all cases at 10 °C min^{-1}.

2.4. Fourier-transform infrared (FT-IR) characterization

The structures of CS, CM and the lyophilized CC dressing were examined using FT-IR spectroscopy, which was performed using an FT-IR spectrometer (Spectrum 2000, Perkin Elmer Co., Norwalk, USA) at ambient conditions. The potassium bromide (KBr) disk technique was used for analysis. Spectra were obtained at a resolution of 2 cm^{-1}, and reported as an average of 16 scans.

2.5. Determination of the swelling properties

The lyophilized and pre-weighed dressing (0.05 g) was immersed in 100 mL of PBS (pH 7.4). At a pre-set time interval, the sample was retrieved by centrifugation for 5 min at a relative centrifugal force of 4,000 × g, followed by the removal of the supernatant. The swelling ratio, water content, and water absorption ratio (WAR) of the sample were calculated. All measurements were repeated three times.

2.6. Evaluation of the erosion behaviour

The erosion behaviour of the dressing was studied as previously described (Lai and Shum, 2015). Briefly, a known mass of a lyophilized dressing was immersed in 100 mL of PBS (pH 7.4), and was incubated at 37 °C. At a pre-set time interval, the sample was retrieved by centrifugation for 5 min at a relative centrifugal force of 4,000 × g, followed by the removal of the supernatant and lyophilization. The ratio between the final dry mass (m) and the initial dry mass (m_o) was calculated. All measurements were repeated three times.

2.7. Scanning electron microscopy (SEM) analysis

The surface morphology of the lyophilized CC dressing was examined using a JEOL JSM-6380 microscope (Tokyo, Japan) operated at an accelerating voltage of 10 kV. Before SEM analysis, the sample was sputter-coated with gold.

2.8. Cytotoxicity assay

3T3 mouse fibroblasts were cultured in DMEM supplemented with 10% FBS, 100 UI/mL penicillin, 100 µg/mL streptomycin, and 2 mM L-glutamine. 24 h before the assay, cells were seeded in a 96-well plate at an initial density of 5000 cells per well, and were incubated under a humidified atmosphere of 5% CO_2 at 37 °C. During the experiment, an appropriate amount of CS, CM, or the lyophilized CC dressing was ground using mortar and pestle, and was re-suspended in the fresh cell culture medium to obtain a suspension with a desired concentration. The suspension was sterilized by filtration with Millipore 0.22 µm syringe filters. The growth medium in each well was replaced with 100 µL of the filtered suspension. After incubating the plate at 37 °C under a humidified atmosphere of 5% CO_2 for 5 h, the suspension in each well was replaced with the fresh cell culture medium. The CellTiter 96 AQueous non-radioactive cell proliferation assay (MTS assay; Promega Corp., Madison, USA) was performed, according to the manufacturer's instructions, either immediately or after 24 h of post-treatment incubation to determine the cell viability (%) in each well. All measurements were repeated three times.

2.9. Rheological measurement

The viscosity of the 4% (w/v) acetic acid solution of CS, the 4% (w/v) aqueous solution of CM, and the CC dressing was measured using the Brookfield DV-III Ultra programmable rheometer (Brookfield

Engineering Laboratories Inc, Middleboro, USA) with spindles (CP-40). Viscosity parameters were determined at different shear rates at ambient conditions, with the equilibration time at every shear rate set as 15 s. Viscoelastic properties of the samples were also examined in the frequency range of 0.1–100 rs^{-1}. The storage modulus (G') and loss modulus (G") were recorded. To examine the changes in the viscoelastic properties of the CC dressing after the drug loading process, MI, MB, and TH were used as drug models. The drug-loaded CC dressing was prepared by first dissolving a drug in a 4% (w/v) aqueous solution of CM to reach a concentration of 12.5 mg/mL. The solution was then mixed with a 4% (w/v) acetic acid solution of CS to reach the CS/CM mass-to-mass ratio of 1:8. The mixture was left at ambient conditions for 5 min for gelation to occur. After that, the G' and G" values were measured.

2.10. Spreadability test

MB was first mixed thoroughly with a 4% (w/v) aqueous solution of CM at a concentration of 7.5 mg/mL, and then mixed with an appropriate volume of a 4% (w/v) acetic acid solution of CS based on the CS/CM mass-to-mass ratio adopted. The mixture was left at ambient conditions for 5 min for gelation to occur. After that, a known mass of the CC dressing was placed on a glass slide. The dressing was spread on the slide using a scraper. The spreadability of different dressings was qualitatively compared.

2.11. Determination of the drug loading efficiency

The drug-loaded CC dressing was prepared as described above. The dressing generated was then lyophilized for two days. 5 mL of distilled water was added to the lyophilized drug-loaded sample. After 30 s of gentle agitation, the sample was retrieved by centrifugation for 5 min at a relative centrifugal force of 16,000 × g. The supernatant was removed. The concentrations of MI, MB, and TH in the supernatant were determined at 280 nm, 665 nm, and 360 nm, respectively, using ultraviolet–visible (UV–Vis) spectroscopy. The drug loading efficiency was calculated. All measurements were repeated three times.

2.12. Drug release evaluation

The drug-loaded CC dressing was prepared as described above. After that, 20 mL of PBS (pH 7.4) was added to the sample. The set-up was incubated at 37 °C under a humidified atmosphere of 5% CO_2. At a pre-set time

interval, 200 μL of PBS was removed for testing, and was replaced with 200 μL of a fresh buffer solution. The amount of the drug released from the sample was determined using UV–Vis spectroscopy as described above. The cumulative drug release was calculated. All measurements were repeated three times.

2.13. In vivo evaluation of the dressing

8-week-old female ICR mice were purchased from Chase Ray Co. Ltd. (Guandzhou, PR China), and were housed in environmentally controlled holding rooms. They were given free access to water and a normal commercial laboratory diet (Purina, Brazil). After a week of environmental adaptation, the mice were randomly divided into four groups of 4 each. The day of the surgical operation was designated as day 0. The surgical procedure was pre-approved by the Ethical Committee of the Hong Kong Polytechnic University. During surgery, the dorsal hair of the mice was shaved using electric clippers, and the shaved area was disinfected with 75% (v/v) ethanol. A round full-thickness wound was made on the back of each animal using a 8 mm biopsy punch. Mice were under isoflurane anaesthesia throughout the surgical procedure. All surgical instruments were sterilized before use. Wounds in the NaCl group and the MI group were treated with 100 μL of a 0.9% (w/v) aqueous solution of NaCl and a 0.25% (w/v) aqueous solution of MI, respectively. Wounds in the CC group were covered by a CC dressing loaded with NaCl (at a concentration of 0.9%); whereas wounds in the CC/MI group were covered by a CC dressing loaded with MI (at a concentration of 0.25%). After that, the mice were bandaged with sterile gauze and a circumferential wrap of cloth tape. The process of wound healing was recorded using a digital camera on day 1, day 4, day 7 and day 10. The size of the wound was measured using Adobe Acrobat Pro. The wound healing rate was calculated.

2.14. Histological analysis

All mice were sacrificed on day 10 after the surgical procedure. A full-thickness skin sample with a 1 cm margin around the wound area was removed from each animal, and was fixed in 4% (v/v) paraformaldehyde in PBS overnight. The tissue sample was embedded in paraffin after dehydration, sectioned at 3-4 μm, and stained with hematoxylin and eosin (H&E) or Masson's trichrome. The stained sections were observed and photographed under a microscope (Leica, Germany). The number of

inflammatory cells and the area percentage of collagen fibers were quantified using Image-J.

2.15. Statistical analysis

All data were expressed as means ± standard deviations (SD). Student's *t*-test was performed to assess the statistical significance. Differences with p-value < 0.05 were considered to be statistically significant.

3. Results and discussion

3.1. Preparation and characterization of the dressing

The CC dressing is generated via electrostatic interactions between the positively charged amine groups of CS and the negatively charged carboxyl groups of CM. The thermal stability of the dressing has been studied using TGA (Fig. 2A). In the TGA curve of the dressing, a significant weight-loss stage is observed at 40–113 °C. It is attributed to the loss of adsorbed and bound water. Another weight loss step occurs at 220–480 °C, owing to the onset of thermal degradation of the polymers. Structural characterization of the dressing has been performed using FTIR (Fig. 2B). The FTIR spectrum of CM shows characteristic bands at 3540, 2903 and 2134 cm^{-1}. They are assigned to the stretching vibration of –OH, –CH and –CO groups, respectively. The characteristic absorption bands of symmetric and asymmetric –COO are observed at 1415 and 1595 cm^{-1}, respectively. These absorption bands are in good agreement with those reported in an earlier study (Su et al., 2010). On the other hand, distinctive absorption bands at 1593 cm^{-1} and 1643 cm^{-1} are detected in the spectrum of CS. These peaks are attributed to the N–H bending vibration (amide II) of a primary amino group and the carbonyl stretching vibration (amide I), respectively (Lee et al., 2004). After gelation, bands at 3400–3301 cm^{-1} broaden. This suggests the occurrence of intermolecular hydrogen bonding between CS and CM.

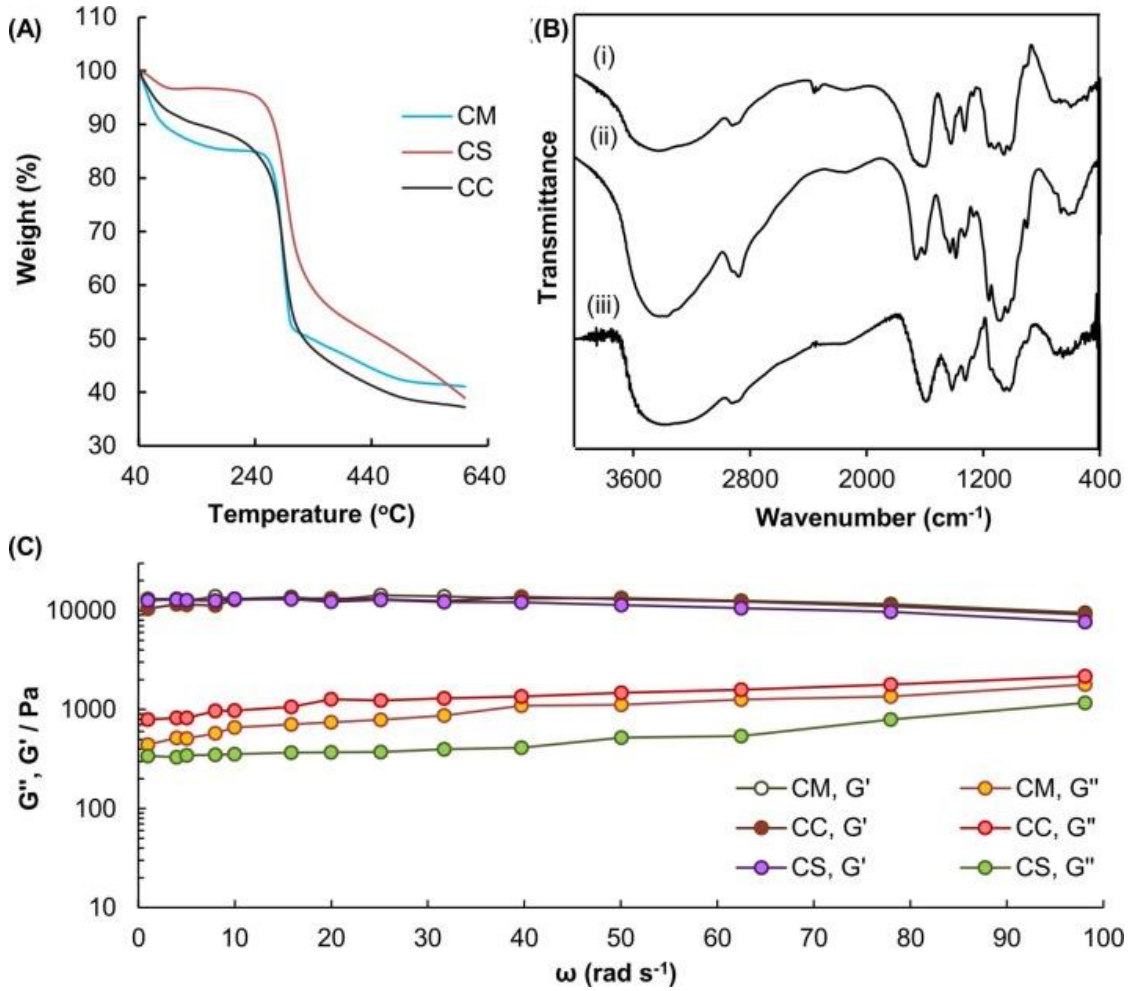

Fig. 2. (A) TGA curves of CM, CS and CC. The CC dressing adopted is CC_{11}. (B) FT-IR spectra of (i) CM, (ii) CS, and (iii) CC. The CC dressing adopted is CC_{11}. (C) Changes in the G" and G' values of different samples (viz., the CM solution, the CS solution, and the CC dressing) from 0.1 to 100 rad s^{-1}. The CC dressing adopted is CC_{11}.

The viscoelastic parameters (i.e., G' and G") of the dressing and its components (CM and CS) are examined by using an oscillatory shear field applied to the samples. The G' and G" values of the dressing are much higher than those of the solutions of CS and CM (Fig. 2C). This is attributed to the fact that electrostatic interactions between CS and CM molecules occur upon mixing. In addition, in the CC dressing, the G' value is higher than the G" value. This implies that the dressing exhibits solid-like behaviour and is robust. CC dressings with different CS mass percentages (3.0%, 11%, and 33%) are generated and designated as CC_{03}, CC_{11} and CC_{33}, respectively. The ratio of amine groups ($-NH_2$) to carboxyl

groups (–COOH) in CC_{03}, CC_{11} and CC_{33} is estimated to be 1:44.4, 1:11.1, and 1:2.8, respectively.

3.2. Swelling capacity and erosion behavior

The swelling capacity of a dressing is one of the important factors determining the release rate of the loaded drug because water in the matrix of the dressing is the medium through which the drug diffuses (Mellott et al., 2001). The swelling capacity of the dressing depends largely on the amount of water the dressing can take up upon hydration, and is closely related to the water content (as well as the swelling ratio and the WAR) of the dressing (Lee et al., 1999, Mellott et al., 2001). Our results show that an increase in the CS/CM ratio causes a decrease in the water content, swelling ratio and WAR of the CC dressing (Fig. 3A–C). Apart from swelling, drug release can be affected by the process of erosion, which is resulted from material degradation that leads to bond cleavage and cross-link dissolution (Zhang & Feng, 2006). As shown in Fig. 3D, the CC dressing with a higher CS mass percentage displays a lower erosion rate owing to a higher extent of electrostatic cross-linking between the CS and CM molecules. This cross-linking restricts the mobility of polymer chains in the CC dressing, thereby offering the dressing generated with a more compact structure, as confirmed by SEM (Fig. 3E). Such a higher compact structure can reduce the swelling capacity and erosion susceptibility of the resultant CC dressing.

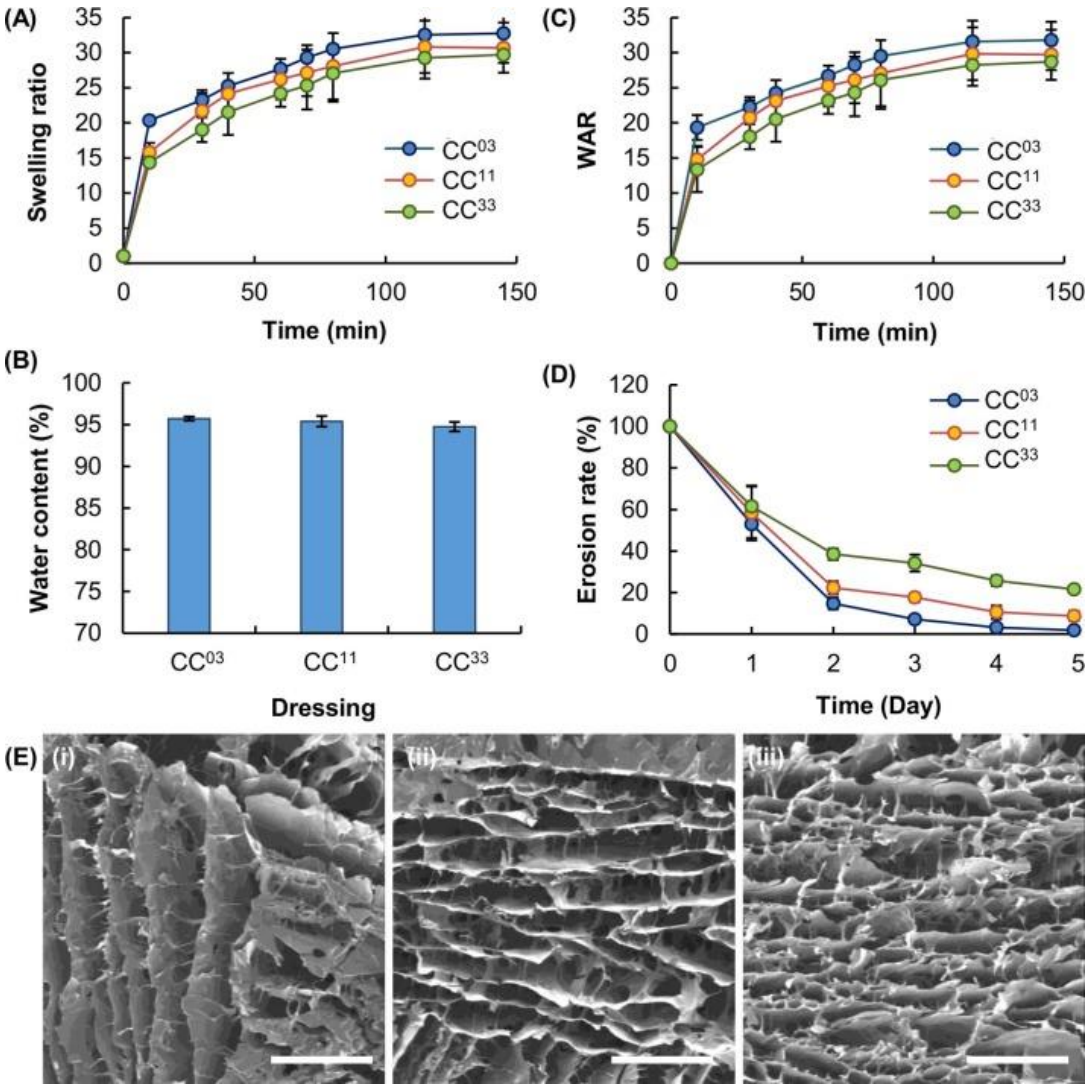

Fig. 3. The (A) swelling ratios, (B) water contents, (C) WARs, and (D) erosion profiles of CC dressings with different CS contents. (E) SEM micrographs of (i) CC^{03}, (ii) CC^{11}, and (iii) CC^{33}. Scale bar = 500 μm.

3.3. Spreadability and rheological properties

The spreadability of a dressing affects the ease of application. As shown in Fig. 4, CC^{11} shows the highest spreadability. This may be because the viscosity of CC^{11} is the lowest among the three CC dressing samples. The low viscosity of CC^{11} is supported by rheological analysis. As shown in Fig. 5A, the apparent viscosity of the CC dressings is higher at a low shear rate than at a high shear rate. This indicates that the dressings exhibit pseudoplastic behaviour. The viscosity of CC^{03} is the highest among all the samples. This is attributed to the high viscosity of CM, which constitutes around 97% of the total mass of the dressing. Compared to CC^{11}, CC^{33} is

more viscous. This is because of the higher mass percentage of CS adopted during the gelation process undertaken by CC_{33}, resulting in a larger amount of amine groups available for forming electrostatic interactions with the carboxyl groups of CM. Changes in C' and C'' values at different shear rates and temperatures are shown in Fig. 5B–C. Results show that the G' values are higher than the G'' values for all samples examined, indicating that the CC dressing displays solid-like behaviour. In addition, no significant change in G' and G'' is observed in the temperature range (30–70 °C) adopted. This suggests that our dressing is thermally stable, with its robustness maintained over a specific temperature range.

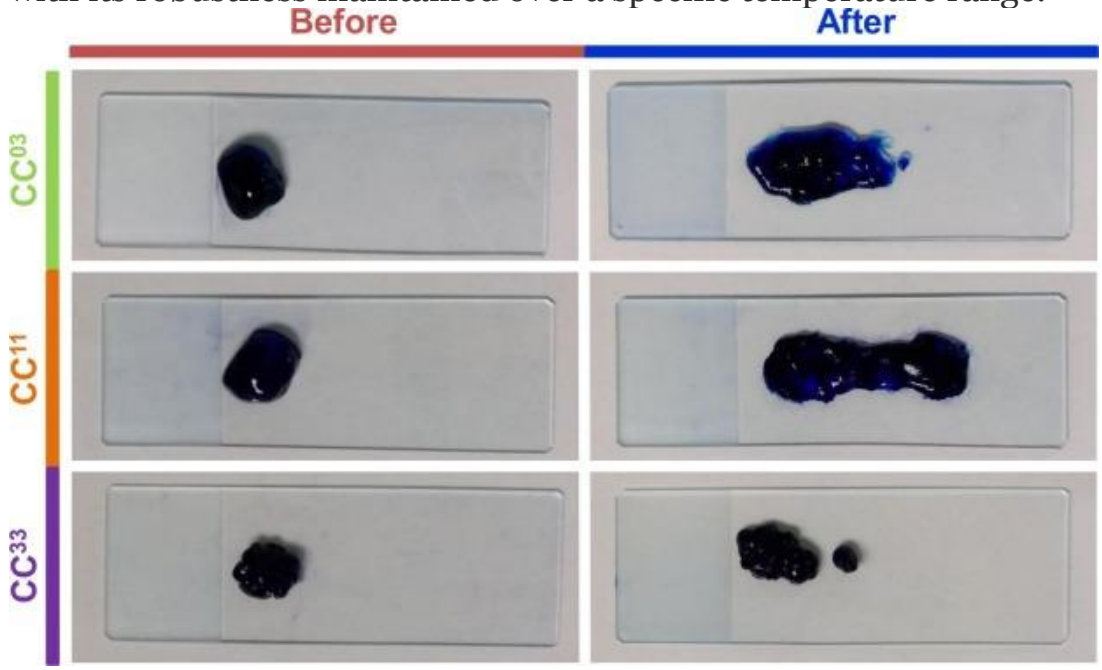

Fig. 4. Photos of MB-loaded CC_{33}, CC_{11}, and CC_{03} dressings before and after spreading.

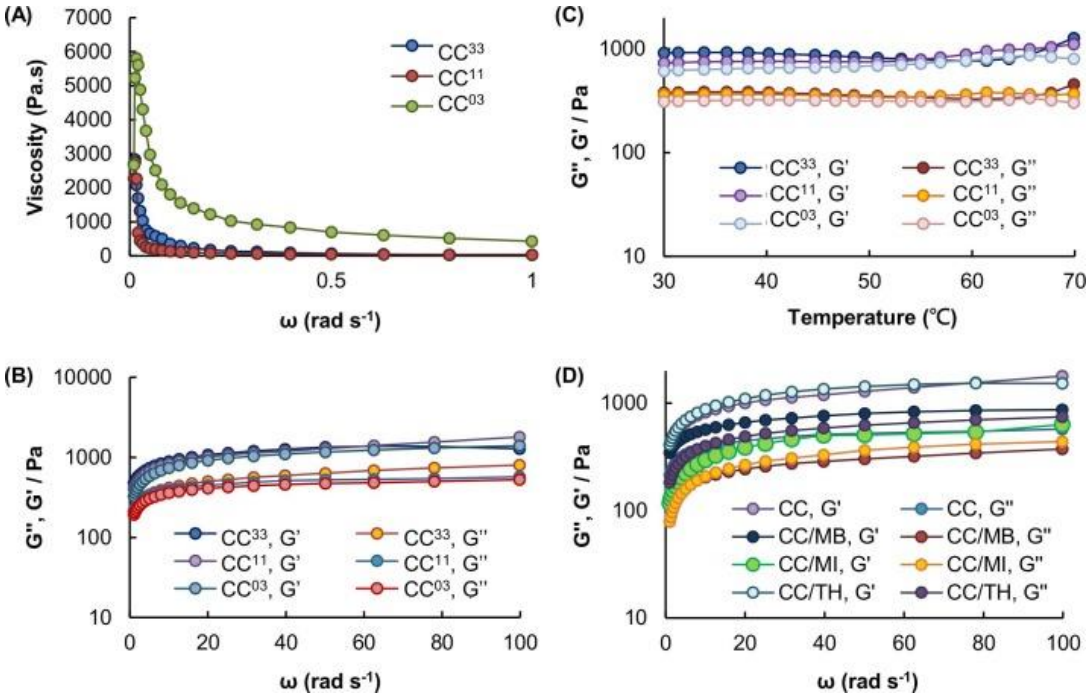

Fig. 5. (A) Changes in the viscosity of different CC dressings from 0.1 to 100 rad s^{-1}. (B) Changes in the G" and G' values of different CC dressings from 0.1 to 100 rad s^{-1}. (C) Changes in the G" and G' values of different CC dressings from 30 to 70 °C. (D) Changes in the G" and G' values of CC^{11}, upon loaded with different drug molecules, from 0.1 to 100 rad s^{-1}.

To examine the effect of the hydrophilicity of drugs on the properties and drug delivery performance of the dressing, MB, MI and TH are selected as drug models because they have similar molecular weights (MB: 319.9 Da; MI: 457.5 Da, TH: 480.9 Da) but very different octanol/water partition coefficients (log K_{ow}) (MB: 5.85; MI: 0.05; TH: −1.37) (National Center for Biotechnology Information Center, 2019a, National Center for Biotechnology Information Center, 2019b, National Center for Biotechnology Information Center, 2019c). After loaded with MB or MI, the C' and C" values of the CC dressing are reduced (Fig. 5D). This is because of the possible interactions between the drug molecules and the charged groups (e.g., $-NH_2$ and –COOH) of polymer chains. This weakens the electrostatic interactions between CS and CM, and hence the strength of the dressing formed. On the other hand, no significant change in the C' and C" values of the CC dressing is observed upon loaded with TH. This is attributed to the fact that TH has the lowest log K_{ow} value among the three drug models examined. Because of the comparatively low hydrophilicity of TH, interactions of the drug molecules with the polymer chains are relatively less. The disruption in electrostatic interactions between CS and CM during gelation can therefore be reduced,

leading to better maintenance of the mechanical strength of the dressing fabricated.

3.4. Evaluation on the drug delivery performance

The cytotoxicity of the CC dressing and its components has been examined using the MTS assay. No significant loss of cell viability is observed after 5 h of treatment with CS, CM and the CC dressing. This indicates that the dressing has negligible acute cytotoxicity (Fig. 6A). To determine the chronic cytotoxicity of the dressing, the viability of the treated cells has been further studied after 24 hours of post-treatment incubation. No detectable cytotoxicity is observed in all concentrations tested. This illustrates the high safety profile of the dressing in biological use.

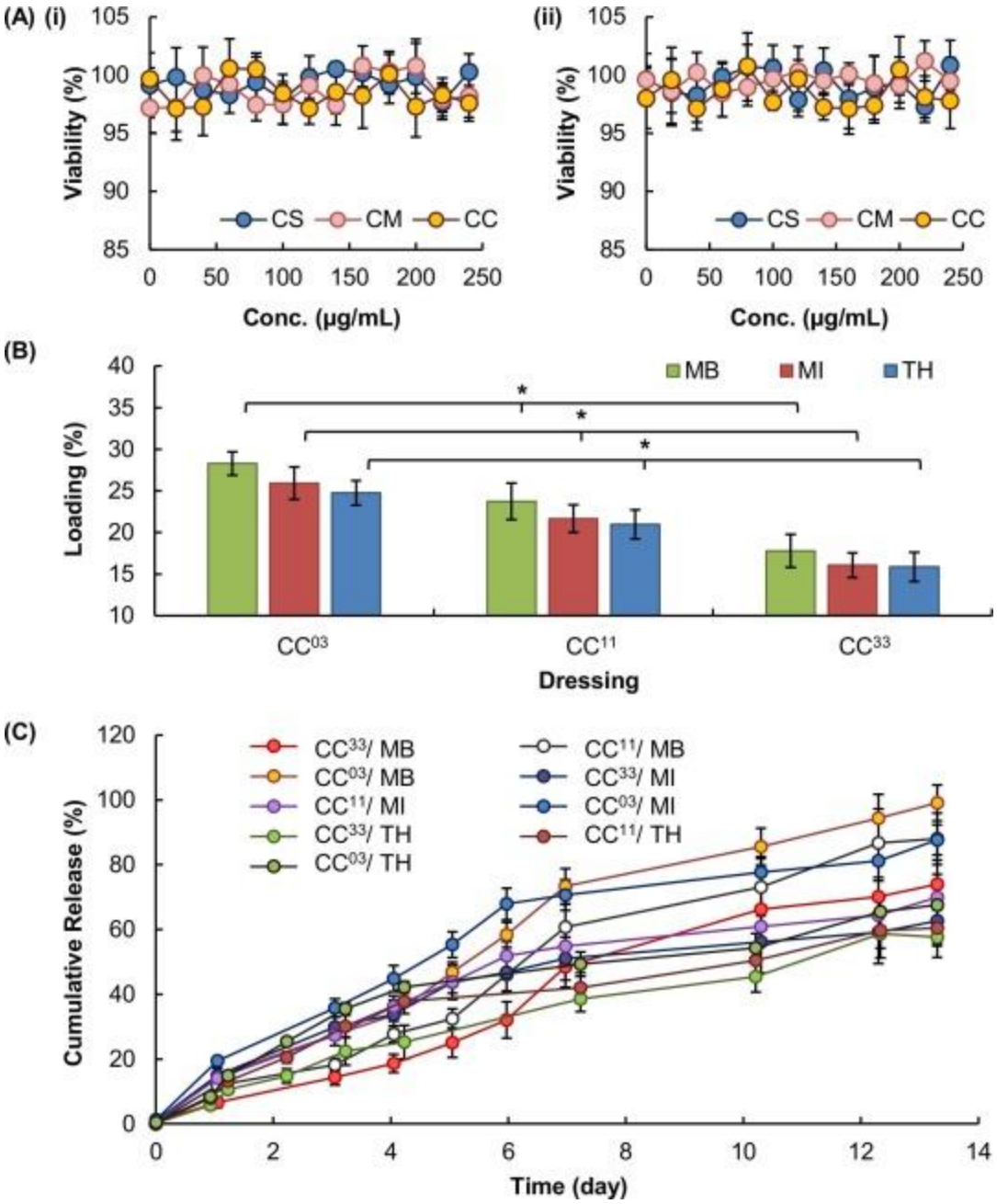

Fig. 6. (A) Viability of 3T3 fibroblasts after treatment with CM, CS and CC, (i) before and (ii) after 24 hours of post-treatment incubation. (B) The loading efficiency of different CC dressings. *$p < 0.05$. (C) Release profiles of the CC dressings loaded with different drugs.

As far as drug loading is concerned, physical entrapment is one of the common methods used in gel systems. Another important method is to chemically conjugate the drug to the carrier (Lai, 2014, Lu et al., 2010, Sun et al., 2017). Compared to chemical conjugation, physical entrapment causes less chemical or biochemical interference to cell

activity and drug action (Zhang et al., 2010), and can minimize structural changes introduced to the loaded drug (Sarkar, 2013, Zhang et al., 2010). In addition, drug loading by physical entrapment does not involve any chemical triggering. This enables the drug loading process to be performed in a simpler and faster manner (Sarkar, 2013). These advantages make physical entrapment a more favourable loading method for fragile or sensitive drugs (Zhang et al., 2010). Our results show that the CC dressing can give a loading efficiency of 20–25%. No significant effect of the hydrophilicity of the drug on the loading efficiency is observed. The drug loading efficiency of the dressing is, however, negatively related to the CS/CM ratio. This may be because an increase in the mass percentage of CM leads to an increase in the viscosity of the dressing, thereby allowing the drug molecules to be held more firmly inside (Fig. 6B).

Compared to CS, CM is more hydrophilic. This explains the observation that the swelling capacity of the dressing increases with the mass percentage of CM (Fig. 3A–C). Changes in the swelling capacity can then affect the release rate of the loaded drug because water in the dressing is the medium through which drug molecules diffuse (Lai et al., 2016). The drug release sustainability of the dressing is, therefore, positively related to the CS mass percentage of the dressing (Fig. 6C). CC_{33} shows the highest drug release sustainability, with only 74% of MB released after 14 days (versus 87% and 99% for CC_{11} and CC_{03}, respectively). The similarly high drug release sustainability of CC_{33} is shown in the other two drug models, with only 60% of TH and 62% of MI released after 14 days. This is attributed to the availability of a large number of amine groups of CS during the gelation process, leading to the formation of a more compact and densely crosslinked dressing that displays lower swelling capacity and lower erosion susceptibility.

3.5. Preclinical evaluation on wound healing

Wound healing is a complicated physiological process, which is roughly divided into four phases: (i) coagulation and haemostasis; (ii) inflammation; (iii) proliferation and (iv) wound remodelling with scar tissue formation (Hunt et al., 2000, Velnar et al., 2009). An ideal wound dressing is the one that can accelerate this process while reducing the pain experienced by patients. Taken its good spreadability and high drug release sustainability into account, CC_{11} is chosen for *in vivo* evaluation (Fig. 7A). By using CC_{11} to deliver MI [which is a semi-synthetic tetracycline possessing antibiotic properties against both gram-positive and gram-negative bacteria (Brenes-Salazar, 2015, Garrido-Mesa et al.,

2013, Joseph et al., 2016), and has been examined clinically for the treatment of skin ulcers (Katsuura et al., 2002)] to the wound in a sustained manner, our objective is to shorten the wound healing time and to reduce the incidence of infection.

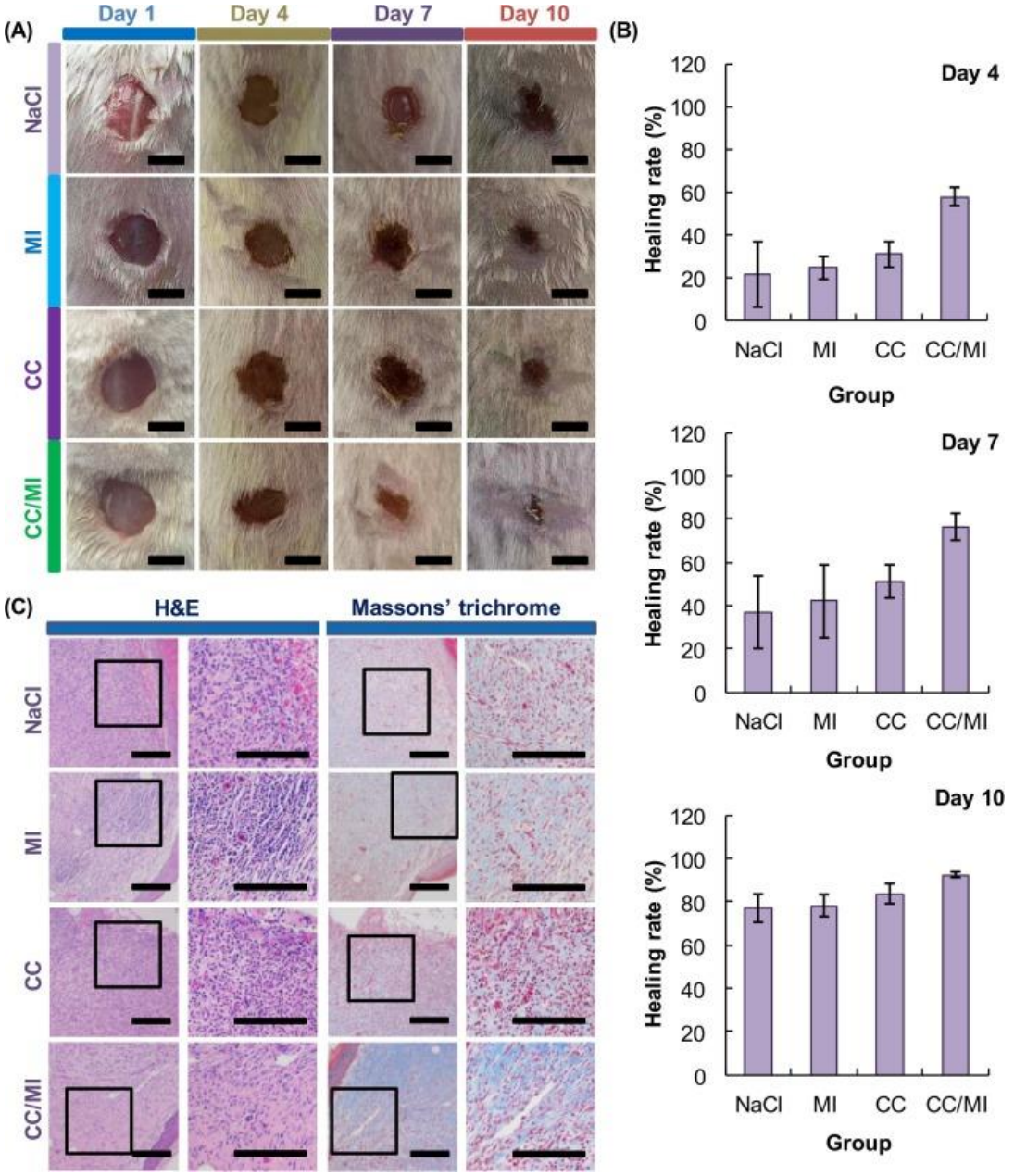

Fig. 7. (A) Photographs of the wounds on day 1, day 4, day 7 and day 10. Scar bar = 5 mm. (B) The wound healing rates of different groups on day 1, day 4, day 7 and day 10. (C) Histological analysis of the wounds on day 10. Sections of the wound tissues are stained with H&E and Masson's trichrome. Selected views in the images are enlarged and put in the right of those images. Scar bar = 100 μm.

In this study, the concentration of MI loaded into the dressing is 0.25% (w/v), which is higher than the reported effective concentration (<0.0003%) of MI for antibacterial activity *in vitro* (Minuth et al., 1974). This concentration has also been previously adopted by Sung *et al.* (Sung et al., 2010), who have loaded a polyvinyl alcohol (PVA)/CS hydrogel with MI to treat wounds in mice and have shown that the concentration of 0.25% is sufficient for wound treatment. Throughout the course of our study, no infection or necrosis in any of the treatment groups has been observed. On day 4, the size of the wound in the CC/MI group is the smallest among all groups tested. On day 7, the size of the wound in the CC/MI group is smaller than that in other groups (i.e., NaCl group, MI group, and CC group), with the onset of tissue regeneration observed. In other groups, the size of the wound, however, is similar to the one on day 4 (Fig. 7B–C). On day 10, the wound in the CC/MI group is almost completely healed, while that in other groups is still in the recovery phase. The MI-loaded CC dressing can facilitate the wound healing process because it can maintain the release of MI in a stable and sustained manner, thereby enhancing the antibacterial effect and shortening the inflammatory stage to induce an earlier onset of the proliferative phase.

To further examine the histomorphologic changes in different groups during the wound healing process, H&E staining and Masson's trichrome staining are used. The relative histomorphometrical values are calculated and are shown in Table 1**.** Compared to other groups, the wound in the CC/MI group shows less inflammatory cell infiltration and more collagen deposition (Fig. 7C). The lower degree of inflammatory cell infiltration indicates that inflammation is less severe in the wound treated with the MI-laoded dressing. The higher level of collagen deposition also suggests that, upon treatment with the MI-loaded dressing, the healing of the wound is promoted.

Table 1. Histomorphometric analysis of the wounds in different groups.

	NaCl group	**MI group**	**CC group**	**CC/MI group**
Number of inflammatory cells†	511.5 ± 79.349	463 ± 119.920	479 ± 136.382	140.6 ± 62.024**
Area percentage of collagen fibers†	25.32 ± 9.765	34.58 ± 5.202	19.233 ± 8.534	62.436 ± 5.864**

† Values are determined based on four randomly selected fields of view of a microscope. The field of view is 0.5 mm x 0.5 mm.

** $p < 0.01$ as compared to the value in the NaCl group.

4. Conclusions

This study reports a CC dressing as a tuneable, biocompatible, and biodegradable system for wound treatment. The dressing is easy to prepare, and shows good spreadability for application. In addition, the swelling and erosion behaviour of the dressing can be manipulated by changing the CS/CM ratio during the gelation process. Such high tunability allows the properties of the dressing to be adjusted to meet the practical needs. Along with its capacity to facilitate wound closure, our dressing warrants further development and optimization for wound healing applications in the clinical context.

Acknowledgments

This project was supported by the University Research Facility for Chemical and Environmental Analysis (UCEA) of PolyU, the HK Polytechnic University Area of Excellent Grants (1-ZVGG), the Natural Science Foundation of Guangdong Province (2018A030310485, and 2018A030313122), and the Shenzhen Science and Technology Innovation Commission (JCYJ20170818102436104, JCYJ20170302144812937, JCYJ20170302145059926, and JCYJ20180305163658916).

Conflict of Interest

The authors declare no conflict of interest.

References

Augustine, R., Dan, P., Schlachet, I., Rouxel, D., Menu, P., Sosnik, A., 2019. Chitosan ascorbate hydrogel improves water uptake capacity and cell adhesion of electrospun poly(epsilon-caprolactone) membranes. Int. J. Pharm. 559, 420–426.

Brenes-Salazar, J.A., 2015. Minocycline: a bacteriostatic antibiotic with pleiotropic cardioprotective effects. Can. J. Physiol. Pharmacol. 93, 863–866.

De Souza, R., Zahedi, P., Allen, C.J., Piquette-Miller, M., 2009. Biocompatibility of injectable chitosan-phospholipid implant systems. Biomaterials 30, 3818–3824.

Escarcega-Galaz, A.A., Sanchez-Machado, D.I., Lopez-Cervantes, J., Sanches-Silva, A., Madera-Santana, T.J., Paseiro-Losada, P., 2018. Characterization data of chitosan- based films: antimicrobial activity, thermal analysis, elementary composition, tensile strength and degree crystallinity. Data Brief 21, 473–479.

Garrido-Mesa, N., Zarzuelo, A., Galvez, J., 2013. Minocycline: far beyond an antibiotic. Br. J. Pharmacol. 169, 337–352.

Hashemi Doulabi, A., Mirzadeh, H., Imani, M., Bagheri-Khoulenjani, S., 2018. Chitosan/polyethylene glycol fumarate blend films for wound dressing application: in vitro biocompatibility and biodegradability assays. Prog. Biomater. 7, 143–150.

Hunt, T.K., Hopf, H., Hussain, Z., 2000. Physiology of wound healing. Adv. Skin WoundCare 13, 6–11.

Jayakumar, R., Prabaharan, M., Sudheesh Kumar, P.T., Nair, S.V., Tamura, H., 2011.Biomaterials based on chitin and chitosan in wound dressing applications. Biotechnol. Adv. 29, 322–337.

Joseph, P., Ponnaiya, J., Das, M., Chaitanya, V.S., Arumugam, S., Ebenezer, M., 2016.Evaluation of anti-bacterial activity of rifapentine, clarithromycin, minocycline,moxifloxacin, ofloxacin and their combinations in murine model of rifampicin re-sistant leprosy. Indian J. Lepr. 88, 147–158.

Katsuura, M., Ikeda, K., Mikajiri, K., Oishi, M., Arakawa, Y., Kataoka, K., Kurokawa, N.,2002. Preparation of a hospital dosage form 0.2% minocycline ointment and accumulation of its drug information. Med. Drug J. 38, 1067–1074.

Lai, W.F., 2014. Cyclodextrins in non-viral gene delivery. Biomaterials 35, 401–411.

Lai, W.F., Shum, H.C., 2016. Hypromellose-graft-chitosan and its polyelectrolyte complex as novel systems for sustained drug delivery. ACS Appl. Mater. Interfaces 7, 10501–10510.

Lai, W.F., Susha, A.S., Rogach, A.L., 2016. Multicompartment microgel beads for co-delivery of multiple drugs at individual release rates. ACS Appl. Mater. Interfaces 8,871–880.

Lee, J.W., Kim, S.Y., Kim, S.S., Lee, Y.M., Lee, K.H., Kim, S.J., 1999. Synthesis and characteristics of interpenetrating polymer network hydrogel composed of chitosan and poly(acrylic acid). J. Appl. Polym. Sci. 73, 113–120.

Lee, S.B., Ha, D.I., Cho, S.K., Kim, S.J., Lee, Y.M., 2004. Temperature/pH-sensitive comb-type graft hydrogels composed of chitosan and poly(N-isopropylacrylamide). J. Appl. Polym. Sci. 92, 2612–2620.

Li, X., Wang, C., Yang, S., Liu, P., Zhang, B., 2018. Electrospun PCL/mupirocin and chitosan/lidocaine hydrochloride multifunctional double layer nanofibrous scaffolds for wound dressing applications. Int. J. Nanomed. 13, 5287–5299.

Lu, X., Ping, Y., Xu, F.J., Li, Z.H., Wang, Q.Q., Chen, J.H., Yang, W.T., Tang, G.P., 2010. Bifunctional conjugates comprising beta-cyclodextrin, polyethylenimine, and 5- fluoro-2'-deoxyuridine for drug delivery and gene transfer. Bioconjug. Chem. 21, 1855–1863.

Mellott, M.B., Searcy, K., Pishko, M.V., 2001. Release of protein from highly cross-linked hydrogels of poly(ethylene glycol) diacrylate fabricated by UV polymerization. Biomaterials 22, 929–941.

Minuth, J.N., Holmes, T.M., Musher, D.M., 1974. Activity of tetracycline, doxycycline, and minocycline against methicillin-susceptible and methicillin-resistant staphylococci. Antimicrob. Agents Chemother. 6, 411–414.

Mishra, S.K., Mary, D.S., Kannan, S., 2017. Copper incorporated microporous chitosan-polyethylene glycol hydrogels loaded with naproxen for effective drug release and anti-infection wound dressing. Int. J. Biol. Macromol. 95, 928–937.

Molla, M.M., Alamgir Hossain, M., Nasrin, T.A.A., Islam, M.N., Sheel, S., 2007. Study on preparation of shelf stable ready to serve (RTS) beverages based on bael pul. Bangladesh J. Agric. Res. 32, 573–586.

National Center for Biotechnology Information, 2019a. PubChem database. Methylene blue, CID=6099. Retrieved April 9, 2019, from https://pubchem.ncbi.nlm.nih.gov/compound/6099.

National Center for Biotechnology Information (2019b). PubChem database. minocycline, CID=54675783. Retrieved April 9, 2019, from https://pubchem.ncbi.nlm.nih.gov/compound/54675783.

National Center for Biotechnology Information (2019c). PubChem database. Tetracycline hydrochloride, CID=54704426. Retrieved April 9, 2019, from https://pubchem.ncbi.nlm.nih.gov/compound/54704426.

Ogushi, Y., Sakai, S., Kawakami, K., 2007. Synthesis of enzymatically-gellable carboxymethylcellulose for biomedical applications. J. Biosci. Bioeng. 104, 30–33.

Pal, K., Banthia, A.K., Majumdar, D.K., 2006. Development of carboxymethyl cellulose acrylate for various biomedical applications. Biomed. Mater. 1, 85–91.

Pena, A., Sanchez, N.S., Calahorra, M., 2013. Effects of chitosan on candida albicans: conditions for its antifungal activity. Biomed Res. Int. 2013, 527549.

Perinelli, D.R., Fagioli, L., Campana, R., Lam, J.K.W., Baffone, W., Palmieri, G.F., Casettari, L., Bonacucina, G., 2018. Chitosan-based nanosystems and their exploited antimicrobial activity. Eur. J. Pharm. Sci. 117, 8–20.

Roller, S., Covill, N., 1999. The antifungal properties of chitosan in laboratory media and apple juice. Int. J. Food Microbiol. 47, 67–77.

Sarkar, D., 2013. Fabrication of an optimized fluorescer encapsulated polymer coated gelatin nanoparticle and study of its retarded release properties. J. Photochem. Photobiol. A Chem. 252, 194–202.

Spera, M.B.M., Taketa, T.B., Beppu, M.M., 2017. Roughness dynamic in surface growth: layer-by-layer thin films of carboxymethyl cellulose/chitosan for biomedical appli- cations. Biointerphases 12, 04E401.

Su, J.F., Huang, Z., Yuan, X.Y., Wang, X.Y., Li, M., 2010. Structure and properties of carboxymethyl cellulose/soy protein isolate blend edible films crosslinked by Maillard reactions. Carbohydr. Polym. 79, 145–153.

Sun, H., Chang, M.Y.Z., Cheng, W.I., Wang, Q., Commisso, A., Capeling, M., Wu, Y., Cheng, C., 2017. Biodegradable zwitterionic sulfobetaine polymer and its conjugate with paclitaxel for sustained drug delivery. Acta Biomater. 64, 290–300.

Sung, J.H., Hwang, M.R., Kim, J.O., Lee, J.H., Kim, Y.I., Kim, J.H., Chang, S.W., Jin, S.G., Kim, J.A., Lyoo, W.S., Han, S.S., Ku, S.K., Yong, C.S., Choi, H.G., 2010. Gel characterisation and in vivo evaluation of minocycline-loaded wound dressing with enhanced wound healing using polyvinyl alcohol and chitosan. Int. J. Pharm. 392, 232–240.

Tamer, T.M., Valachova, K., Hassan, M.A., Omer, A.M., El-Shafeey, M., Mohy Eldin, M.S., Soltes, L., 2018. Chitosan/hyaluronan/edaravone membranes for anti-inflammatory wound dressing: in vitro and in vivo evaluation studies. Mater. Sci. Eng. C Mater. Biol. Appl. 90, 227–235.

Velnar, T., Bailey, T., Smrkolj, V., 2009. The wound healing process: an overview of the cellular and molecular mechanisms. J. Int. Med. Res. 37, 1528–1542.

Vinklarkova, L., Masteikova, R., Foltynova, G., Muselík, J., Pavlokova, S., Bernatoniene, J., Vetchya, D., 2017. Film wound dressing with local anesthetic based on insoluble carboxymethycellulose matrix. J. Appl. Biomed. 15, 313–320.

Wang, P., He, H., Cai, R., Tao, G., Yang, M., Zuo, H., Umar, A., Wang, Y., 2019. Cross-linking of dialdehyde carboxymethyl cellulose with silk sericin to reinforce sericin film for potential biomedical application. Carbohydr. Polym. 212, 403–411.

Zhang, D., Zhou, W., Wei, B., Wang, X., Tang, R., Nie, J., Wang, J., 2015. Carboxyl-modified poly(vinyl alcohol)-crosslinked chitosan hydrogel films for potential wound dressing. Carbohydr. Polym. 125, 189–199.

Zhang, X.L., Huang, J., Chang, P.R., Li, J.L., Chen, Y.M., Wang, D.X., Yu, J.H., Chen, J.H., 2010. Structure and properties of polysaccharide nanocrystal-doped supramolecular hydrogels based on cyclodextrin inclusion. Polymer 51, 4398–4407.

Zhang, Z.P., Feng, S.S., 2006. Nanoparticles of poly(lactide)/vitamin E TPGS copolymer for cancer chemotherapy: synthesis, formulation, characterization and in vitro drug release. Biomaterials 27, 262–270.

W.-F. Lai, et al. International Journal of Pharmaceutics 566 (2019) 101–110